JOURNAL OF CATALYSIS 112, 66–79 (1988)

Acidity of Unsupported and Silica-Supported Vanadia, Molybdena, and Titania as Studied by Pyridine Adsorption

TAKUO KATAOKA[1] AND J. A. DUMESIC[2]

Department of Chemical Engineering, University of Wisconsin, Madison, Wisconsin 53706

Received August 18, 1987; revised January 26, 1988

The acidic properties of unsupported titania, vanadia, and molybdena, and the corresponding silica-supported metal oxides were studied. The number of acid sites was investigated by thermogravimetry of adsorbed pyridine. The types of acid sites were examined by infrared spectroscopy of adsorbed pyridine. Both Lewis and Brønsted acid sites were present on the surfaces of V_2O_5 and MoO_3, while Lewis acid sites were found exclusively for TiO_2. When supported on silica, vanadia and molybdena species showed a greater number of acid sites than the corresponding unsupported oxides. The oxidized surfaces of these materials possessed both Lewis and Brønsted acid sites. In contrast, Lewis sites predominated on the surfaces of the reduced samples. Silica-supported titania showed strong Lewis acidity, analogous to unsupported titania. The addition of water vapor was observed to generate Brønsted acid sites for the oxidized forms of silica-supported titania, vanadia, and molybdena. This behavior was not observed for the reduced forms of these materials. Pauling's electrostatic bond strength rules are shown to be useful to predict whether Brønsted acid sites exist on the surfaces of metal oxides.

INTRODUCTION

Metal oxides are important catalytic materials for the production of a variety of valuable chemicals such as dienes, aldehydes, and acid anhydrides. Vanadia, molybdena, and titania are often important components for such catalytic materials, e.g., for the conversion of *n*-butane to maleic anhydride and the reaction of *o*-xylene to phthalic anhydride (*1–3*). In addition, titania-supported vanadia has been found to be an active catalyst for the reduction of NO_x emissions from stationary sources (*4, 5*). Recently, silica-supported molybdena and vanadia have been shown to be effective catalysts for the partial oxidation of methane to formaldehyde (*6, 7*). Due to the importance of vanadia, molybdena, and titania in the aforementioned catalytic processes, the present study was undertaken to probe the surface properties of these materials.

In general, the catalytic behavior of metal oxides may be described in terms of acid/base concepts and oxidation/reduction properties. For example, the acid/base properties of the catalyst may be important for the adsorption and activation of organic reactants. The oxidation/reduction properties of the catalyst are important for the selective incorporation of oxygen into the reactant molecules. The present study focuses on the acid properties of selected metal oxides; however, it also includes the study of the effects of catalyst oxidation state on acid/base properties.

The acid properties of mixed metal oxides have been studied by a variety of authors (e.g., *8–29*). The comparison of results between different investigations, however, is generally difficult due to different types of samples studied, different sample treatments employed, and different techniques used to measure acidity. In previous studies, we have investigated the acidic properties of silica-supported Sc, Al, Ga, Mg, Zn, and Fe oxides (*30–32*). The first three silica-supported oxides displayed both Lewis and Brønsted acidities, while

---

[1] Present address: Toho Titanium Co., 3-3-5 Chigasaki, Kanagawa 253, Japan.

[2] To whom correspondence should be addressed.

0021-9517/88 $3.00

the latter three showed only Lewis acid sites. Furthermore, silica was shown to stabilize supported metal cations in sites of low coordination, thereby leading to acid sites. We have studied silica-supported vanadia, molybdena, and titania in the present study to probe the factors responsible for the generation of Brønsted acid sites and to study the effects of the silica support on the acidic properties of these materials. These studies were carried out under the same conditions as those used in our previous work so that the results of all studies can be compared and contrasted.

EXPERIMENTAL

The experimental techniques employed in the present work to investigate the acidic properties of metal oxides include thermogravimetry and infrared spectroscopy of adsorbed pyridine. The number of acid sites was determined as the amount of irreversibly adsorbed pyridine at progressively higher temperatures. The type of acid sites was examined by infrared spectra of adsorbed pyridine, as proposed originally by Parry (*33*). An outline of the experimental methods is presented below.

Sample Preparation

The samples studied in this investigation of acidity were unsupported SiO_2, TiO_2, V_2O_5, and MoO_3, as well as silica-supported titania, vanadia, and molybdena. Some studies were also conducted on silica-supported alumina and zinc oxide. The silica (CAB-O-SIL, S-17) was used as received, and it had a surface area of 370 m^2/g. The titania (Degussa, P25) was cleaned prior to use by the method described by Santos *et al.* (*34*), and its surface area was 54 m^2/g. Vanadia was prepared by the thermal decomposition at 720 K of ammonium metavanadate (Aldrich), leading to a surface area of 8.7 m^2/g. Molybdena was prepared in a similar fashion starting with ammonium molybdate (Mallinckrodt), and its final surface area was 10.1 m^2/g.

The silica-supported samples were prepared by incipient wetness impregnation, using 1 ml of solution per gram of silica. The Ti/SiO_2 (1.01 wt% Ti) sample was prepared in a dry box using a hexane solution of titanium isopropoxide, following the method of Chien (*35*). The V/SiO_2 sample (1.03 wt% V) was prepared with an oxalic acid solution of ammonium metavanadate, and Mo/SiO_2 samples (1.00 and 6.41 wt% Mo) were prepared using aqueous solutions of ammonium molybdate. Silica-supported alumina and zinc oxide samples were prepared using the appropriate nitrate salts, as described in previous investigations (*30–32*); these two samples contained 0.26 and 0.52 wt% of the supported metal cations, respectively.

Thermogravimetry

Gravimetric measurements of adsorbed pyridine were carried out using a conventional vacuum system equipped with a quartz-spring balance. The spring was surrounded by a water jacket kept at constant temperature (300 K). A sample of ca. 450 mg was pressed into a 10-mm-diameter pellet and was placed on a quartz bucket suspended by the spring. After the sample was oxidized or reduced, the system was evacuated at 720 K for 1 h, or until the pressure reached below 1×10^{-4} Torr. At this point, the dry weight of the sample was measured. After cooling to a temperature of 420 K, 4.8 Torr of pyridine was introduced into the apparatus for 1 h. The system was then evacuated at 420 K until the pressure reached 3×10^{-5} Torr. At this point, the amount of adsorbed pyridine was determined at room temperature. In a similar manner, the sample was heated under vacuum to 520, 620, and 720 K, and the corresponding amounts of adsorbed pyridine were measured.

Infrared Spectroscopy

All spectra were recorded at room temperature using a Nicolet 7199 Fourier transform infrared spectrometer, operated with a resolution of 2 cm^{-1}. Transmission infrared spectroscopy was employed for most of the samples. Samples of 40 mg were made into the form of thin wafers and mounted in a stainless-steel holder in the cell. The cell was so designed that the holder could move from a Pyrex portion of the cell where the sample could be heated to an aluminum section where a pair of CaF_2 windows were attached to allow collection of the spectra. Diffuse reflectance spectroscopy was employed for MoO_3 and V_2O_5 because of the low transparency of these samples. Samples were loosely pressed into the form of a pellet and placed on a platform below a CaF_2 window attached to the glass diffuse reflectance cell. Both infrared cells are described elsewhere (*36*).

The samples were treated in O_2 or H_2 at 720 K followed by evacuation to 1×10^{-4} Torr at the same temperature. The spectrum of each sample was then recorded at room temperature. After the adsorption of 4.8 Torr of pyridine at 420 K, the system was evacuated at progressively higher temperatures to 1×10^{-4} Torr, unless otherwise noted. The spectrum of the sample alone was subtracted from that of the sample with adsorbed pyridine for each case. The effects of water were investigated in separate runs. In short, 7 Torr of water vapor was admitted into the cell at room temperature after evacuation of the preadsorbed pyridine at 420 K, and the spectrum was then recorded. The system was further evacuated to 1×10^{-4} Torr while heating to 420 K, and another spectrum was taken. The corresponding spectrum of the sample alone with adsorbed water was also collected separately and subtracted from that of the sample with adsorbed pyridine and water.

Chemicals

Pyridine (Aldrich, spectroscopic grade) was purified by a freeze–pump–thaw method prior to use, and it was stored in a glass bulb containing activated molecular sieve (3A). Oxygen (Matheson) and hydrogen (Airco) were passed through activated molecular sieves (13×) cooled with dry ice–acetone and liquid nitrogen, respectively. A Deoxo catalytic purifier (Fisher Scientific) was also employed upstream of the molecular sieve trap for hydrogen purification.

RESULTS

Unsupported Oxides

Approximately 7×10^{15} molecules/m^2 of pyridine remained on the surface of silica after evacuation at 420 K, corresponding to ca. 0.1% of the surface, and this small amount completely desorbed at 520 K. The sample evacuated at 420 K revealed the 19b and 8a modes of adsorbed pyridine at 1446 and 1598 cm^{-1}, respectively, which have been ascribed to hydrogen-bonded pyridine (e.g., see discussion in Refs. (*30–32*)). No Brønsted acid sites were observed, as revealed by the absence of a pyridinium band at 1550 cm^{-1}.

The amount of pyridine adsorbed on titania at 420 K is equivalent to 20% of the surface. Even after evacuation at 720 K, some of the pyridine remains on the surface, suggesting that titania is highly acidic. Figure 1 shows infrared spectra of adsorbed pyridine. The characteristic absorption peaks of pyridine adsorbed on Lewis acid sites appear at 1446, 1493, 1576, and 1606 cm^{-1} after evacuation at 420 K. There is no evidence for the presence of Brønsted acid sites. When the sample is subsequently exposed to water vapor, the intensity of the 19b peak decreases to almost one-half the intensity of that in spectrum A. This may be an indication of an interaction of surface cations with water, which causes some of the adsorbed pyridine to be displaced. In fact, a new peak appears at 1596 cm^{-1}, characteristic of hydrogen-bonded pyridine. No Brønsted acid sites were observed, which is in agreement with the literature (*37*).

At 420 K, the amount of adsorbed pyridine on vanadia corresponds to only 2% of the surface, as calculated from an estimated

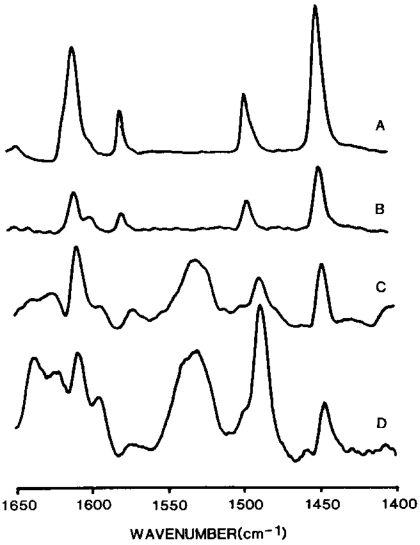

FIG. 1. Infrared spectra of pyridine adsorbed on oxidized TiO_2 and V_2O_5. (A) Pyridine adsorbed on TiO_2 after evacuation at 420 K, 10^{-4} Torr; (B) sample subsequently exposed to 7 Torr of water vapor at room temperature; (C) pyridine adsorbed on V_2O_5 after evacuation at 420 K, 10^{-3} Torr; (D) sample subsequently exposed to 7 Torr of water vapor at room temperature.

cross-sectional area of a surface VO_4 unit equal to 0.10 nm^2. As the evacuation temperature was raised, the amount of adsorbed pyridine approached zero at 520 K. Diffuse reflectance infrared spectra of adsorbed pyridine are given in Fig. 1. Spectrum C was taken after evacuation to 5×10^{-3} Torr at 420 K. The characteristic absorption peaks of pyridine on Lewis acid sites appear at 1448 and 1609 cm^{-1}, and a peak due to adsorption on Brønsted acid sites appears at 1531 cm^{-1}. After spectrum C was taken, water vapor was admitted into the system and spectrum D was recorded. The intensity of the peak at 1531 cm^{-1} increased, while the peak at 1448 cm^{-1} became weaker, suggesting that additional Brønsted acid sites have been generated at the expense of Lewis acid sites. The peak at 1597 cm^{-1} is due to hydrogen-bonded pyridine. Upon further evacuation, the absorption peak for pyridine on Brønsted acid sites decreased, accompanied by an increase in that for Lewis acid sites. The observation of Brønsted acidity is consistent with the literature (*38, 39*).

The amount of pyridine remaining on molybdena after evacuation at 420 K corresponds to 5% of the surface, as calculated using 0.15 nm^2 for the cross-sectional area of a surface MoO_4 unit. At temperatures above 520 K, no pyridine remained on the surface. The diffuse reflectance infrared spectra of adsorbed pyridine are similar to those for pyridine on vanadia. Both Lewis acid sites and Brønsted acid sites are observed, even in the absence of water vapor. According to Belokopytov *et al.* (*38*), outgassing at 473 K completely eliminates the characteristic absorption bands of adsorbed ammonia on MoO_3, while adsorption of water creates additional Brønsted sites which do not disappear upon evacuation at room temperature. The present observations are in accord with their results.

It should be noted that the unsupported TiO_2, V_2O_5, and MoO_3 samples were studied only in their oxidized states, since these samples became highly absorbant to infrared light upon reduction.

Silica-Supported Oxides

An oxidized sample of Ti/SiO_2 was obtained by treating the material in flowing oxygen at 720 K overnight. A reduced sample was prepared by subsequent treatment in flowing hydrogen at 720 K for 6 h. For both the oxidized and the reduced samples, the amount of adsorbed pyridine was 4×10^{16} molecules/m^2 following evacuation at 420 K, which corresponds to 12% of the dopant cations. At higher evacuation temperatures, more pyridine was found to remain on the oxidized sample. Strong acid sites may exist on the Ti/SiO_2 samples, since some adsorbed pyridine remains even at 720 K.

Infrared spectra of adsorbed pyridine on the oxidized Ti/SiO_2 sample showed that only Lewis acid sites were present on the surface. Similar spectra were observed for

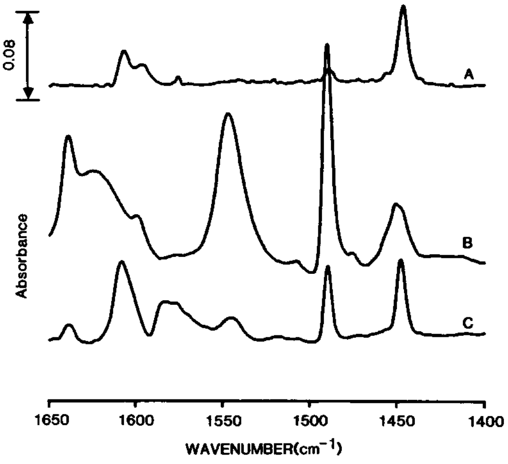

FIG. 2. Infrared spectra of pyridine adsorbed on oxidized Ti/SiO$_2$. (A) Pyridine adsorbed after evacuation at 420 K, 10^{-4} Torr; (B) sample subsequently exposed to 7 Torr of water vapor at room temperature; (C) following evacuation at 420 K, 10^{-4} Torr.

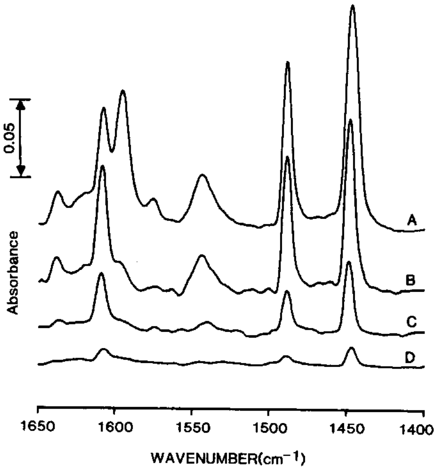

FIG. 3. Infrared spectra of pyridine adsorbed on oxidized V/SiO$_2$. (A) After evacuation at 420 K, 10^{-3} Torr; (B) after evacuation at 420 K, 10^{-4} Torr; (C) after evacuation at 520 K, 10^{-4} Torr; (D) after evacuation at 620 K, 10^{-4} Torr.

the reduced sample. The effects of water on the acidic properties can be seen in the infrared spectra of Fig. 2. When the oxidized sample, on which pyridine had been preadsorbed, was contacted with water vapor at room temperature, a significant number of Brønsted acid sites was generated. However, the strength of the Brønsted acidity seems to be weak, as evidenced by the decrease in the intensity of the peak at 1545 cm^{-1} upon evacuation at 420 K. On the other hand, no Brønsted acidity was observed for the reduced sample, even when the sample was exposed to water vapor.

An oxidized sample of V/SiO$_2$ was prepared by treatment of the material in flowing oxygen at 720 K overnight. A reduced sample was made by subsequent treatment in flowing hydrogen at 720 K for 6 h. The extent of pyridine adsorption was higher on the reduced sample than on the oxidized sample over the entire temperature range. The amount of adsorbed pyridine after evacuation at 420 K corresponds to 19% of the added cations in the former case, and 7.8% in the latter case.

Infrared spectra of adsorbed pyridine are shown in Figs. 3 and 4. The characteristic absorption bands of pyridine adsorbed on Lewis acid sites and on Brønsted acid sites are seen on the oxidized sample. The intensity of the peak near 1545 cm^{-1} decreases with increasing evacuation temperatures; however, it is still observable even at 620 K. It can be concluded that the Brønsted

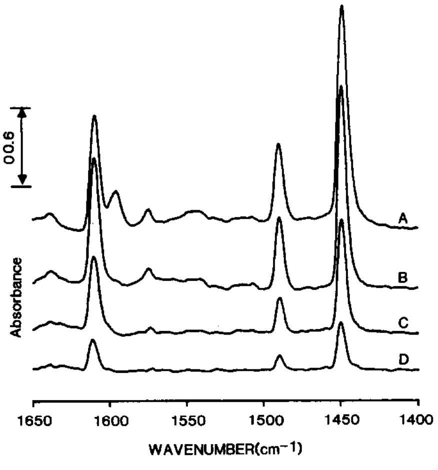

FIG. 4. Infrared spectra of pyridine adsorbed on reduced V/SiO$_2$. (A) After evacuation at 420 K, 10^{-3} Torr; (B) after evacuation at 420 K, 10^{-4} Torr; (C) after evacuation at 520 K, 10^{-4} Torr; (D) after evacuation at 620 K, 10^{-4} Torr.

acidity on the oxidized V/SiO_2 is strong, compared to the other supported oxides used in this work. The presence of Lewis acid sites was found to be predominant for the reduced sample. A small amount of Brønsted acidity seems to exist at temperatures below 420 K.

The infrared spectra of adsorbed pyridine in the presence of water vapor for oxidized V/SiO_2 revealed a considerable increase in the Brønsted acidity for the oxidized sample upon water adsorption, as indicated by an increase in the intensity of the peak at 1545 cm^{-1}. On the reduced sample, however, the adsorption of water appeared to generate only a small number of Brønsted acid sites.

Oxidized samples of Mo/SiO_2 were prepared by treatment in flowing oxygen at 720 K overnight. Reduced samples were generated by subsequent treatment in flowing hydrogen at 720 K for 6 h. The results of gravimetric adsorption of pyridine on the 1 wt% Mo/SiO_2 sample at varying evacuation temperatures were similar to those for V/SiO_2. The amount of adsorbed pyridine at 420 K corresponds to 12% of the dopant cations for the oxidized sample, and 19% for the reduced sample.

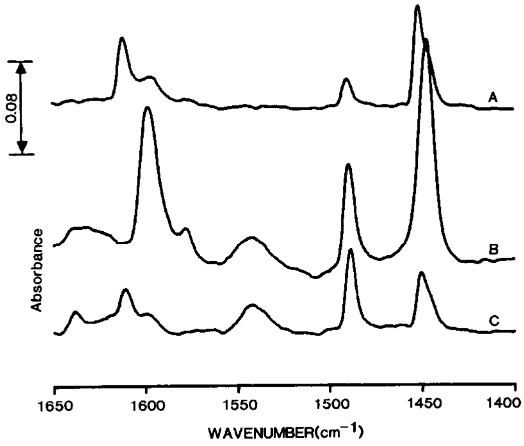

FIG. 5. Infrared spectra of pyridine adsorbed on oxidized 1.0 wt% Mo/SiO_2. (A) Pyridine adsorbed after evacuation at 420 K, 10^{-4} Torr; (B) sample subsequently exposed to 7 Torr of water vapor at room temperature; (C) following evacuation at 420 K, 10^{-4} Torr.

Infrared spectra of adsorbed pyridine on the oxidized 1 wt% sample showed only Lewis acid sites. Similar spectra were observed for the reduced sample. The effects of water on the infrared spectra of adsorbed pyridine on the oxidized sample are shown in Fig. 5. Although only Lewis acidity was observed in the absence of water, Brønsted acid sites were formed upon water adsorption. The effect was more dramatic for the oxidized sample. The conversion of pyridine adsorbed on Lewis acid sites to hydrogen-bonded pyridine is also evident.

Infrared spectra of adsorbed pyridine on the 6.4 wt% Mo/SiO_2 sample were also collected for the oxidized sample after pyridine adsorption. Although only Lewis acid sites were observed on 1 wt% Mo/SiO_2 under water-free conditions, small amounts of Brønsted acid sites were found to exist for the 6.4 wt% Mo/SiO_2 sample. Observations similar to those in the present study have been reported by Kiviat and Petrakis for oxidized molybdenum oxide supported on alumina, where evidence for protonated pyridine first appeared when the loading exceeded 6 wt% (*24*). The effects of water on the generation of Brønsted sites for alumina-supported molybdena have also been documented (*24*, *27*).

An oxidized sample of Al/SiO_2 was prepared by treatment in oxygen at 720 K. The results of thermogravimetric studies of this sample have been reported elsewhere (*32*). Infrared spectra of adsorbed pyridine collected before and after water exposure are shown in Fig. 6. It is known that Al/SiO_2 possesses both Lewis and Brønsted acid sites (e.g., (*33*)). As shown in spectrum A, Brønsted acid sites are present even in the absence of water. When the sample is contacted with water vapor at room temperature, it is seen that the Brønsted acidity is enhanced, with a concomitant transformation of pyridine adsorbed on Lewis acid sites into hydrogen-bonded pyridine (spectrum B). Even after further evacuation at 420 K, the intensity of the peak at 1547 cm^{-1} does not decrease (spectrum C),

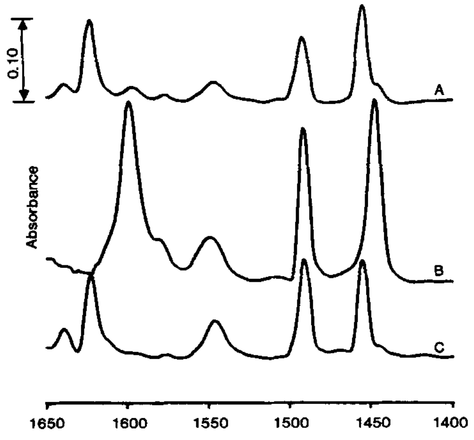

FIG. 6. Infrared spectra of pyridine adsorbed on oxidized Al/SiO_2. (A) Pyridine adsorbed after evacuation at 420 K, 10^{-4} Torr; (B) sample subsequently exposed to 7 Torr of water vapor at room temperature; (C) following evacuation at 420 K, 10^{-4} Torr.

which suggests that the induced Brønsted acidity is strong.

An earlier study reported the results of thermogravimetric measurements of pyridine adsorption on an oxidized Zn/SiO_2 sample (*32*). Infrared spectra collected in the present study of pyridine adsorbed on this sample showed only Lewis acid sites, even for the sample contacted with water vapor.

DISCUSSION

Unsupported Oxides

It was observed in the present study that the number of acid sites per unit surface area was significantly larger for oxidized titania than for vanadia, molybdena, and that silica did not possess a detectable number of acid sites (as measured by pyridine adsorption). In a previous study (*32*), it has been suggested that the Lewis acidity of a metal oxide can be correlated with the Sanderson electronegativity of the oxide. Specifically, oxides with low electronegativities such as magnesia are not acidic; materials with higher electronegativities such as alumina and titania display significant numbers of Lewis acid sites; and oxides with high electronegativities such as silica may not display appreciable Lewis acidity due to the absence of coordinatively unsaturated metal cations on the surface.

We must now extend the above ideas to include the result of the present study that oxidized vanadia and molybdena do not show large numbers of Lewis acid sites, despite the fact that the Sanderson electronegativities of these oxides are similar to those of alumina and titania. The origin of this behavior may be that vanadia and molybdena exist as layered oxides (e.g., (*40–44*)), containing doubly bonded oxygens at the surface. Accordingly, it is possible to form cleavage planes for these oxides in which the vanadium or molybdenum cations are coordinatively saturated and as such these cations would not form strong Lewis acid centers. Of major importance is the observation that vanadia and molybdena display significant Brønsted acidity, while alumina and titania do not. This will be addressed below.

Silica-Supported Oxides

It is known that Ti/SiO_2 possesses strong acidity (*45, 46*). In the present study, the acid sites were shown to be of Lewis type in the absence of water vapor. The Lewis acidity of the oxidized surface was found to become weaker upon reduction of the sample. Such a decrease in the acidity upon reduction may be attributable to the decrease in cation charge and electronegativity.

At the lower loading of Mo on silica, the number of sites was found to increase upon reduction, while the amount of adsorbed pyridine at 420 K was greater on the oxidized sample than on the reduced sample at the higher Mo loading. It has been pointed out that polymeric molybdenum species or crystalline MoO_3 can be readily formed on silica, even below monolayer coverage. Marcinkowska *et al.* (*47*), for example, reported that the crystalline species, as detected by Raman spectroscopy, was formed at a Mo loading of 2 wt% for a sample prepared by incipient wetness impregnation. Iwasawa and Yamagishi (*48*) found that at least three types of Mo in different environments are present on impregnated Mo/SiO_2, even at Mo contents below 1 wt%.

When a Mo/SiO_2 sample is subjected to reduction, the oxidation state of Mo ion is likely to become Mo^{5+} or Mo^{4+} under the conditions studied (*49, 50*). In the case where Mo^{4+} is formed, the reduction scheme proposed by Yermakov *et al.* (*51, 52*) may be applicable at low Mo loadings, for which the cation would be surrounded by three oxygens. A similar model has been established for the reduced state of Mo/Al_2O_3 (*53*). The surface cations in this environment are coordinatively unsaturated, leading to Lewis acid sites. In this regard, the number of Lewis acid sites on Mo/SiO_2 with low Mo loadings may be higher in the reduced state than in the oxidized state. At higher Mo loadings, on the other hand, Mo^{6+} ions on the silica surface are expected to be present primarily as interconnecting MoO_6 octahedra. The removal upon reduction of oxygens interconnecting two Mo ions may in part lead to the formation of Mo–Mo bonds, due to the relatively close separation of molybdate units. The existence of metal-to-metal bonds is well documented in the structure of MoO_2, and it has also been proposed to occur on reduced Mo/Al_2O_3 (*54*). Since coordinative unsaturation caused by reduction is alleviated by forming metal–metal bonds between cations, the number of Lewis acid sites can be smaller in the reduced than in the oxidized form.

The number of acid sites on V/SiO_2 was larger on the reduced sample than on the oxidized sample. Van Reijen and Cossee (*55*) advocated that the VO_4 units on silica are capable of adsorbing electron donors by altering their coordination spheres from tetrahedral to square pyramidal. In the present study, only weak acidity was found on the oxidized sample; therefore, the electron attracting force of the surface VO_4 unit is apparently not very strong. On the other hand, reduction would cause the removal of terminal and/or bridging oxygens, thereby creating surface anion vacancies as in the case of Mo/SiO_2. Hence, an increase in the acidity upon reduction is expected, in agreement with the experimental results. Importantly, Brønsted acid sites were observed in the present study of oxidized V/SiO_2, even in the absence of water vapor. This will be discussed in a separate section.

Generation of Brønsted Acid Sites

The importance of Brønsted acidity in reactions such as catalytic cracking and isomerization of hydrocarbons has been recognized in many works. An accepted model accounting for the Lewis and Brønsted acid sites of silica–alumina is that an aluminum ion is incorporated in the tetrahedral network of a SiO_2 unit (e.g., (*56*)). In the dehydrated form, Al^{3+} is bound to three oxygens, rendering coordinative unsaturation which leads to Lewis acidity. In the hydrated state, the Al ion completes its tetrahedral coordination sphere. The presence of a trivalent cation in a tetrahedral site, coordinated to oxygen anions that are shared between two cations, leads to a formal charge of -1. A proton is required to satisfy electrical neutrality, which originates from a bridging hydroxyl group. This leads to Brønsted acidity. For a series of cations doped onto silica, Connell and Dumesic demonstrated the validity of the above model for not only Al^{3+} but also other trivalent cations such as Sc^{3+} and Ga^{3+} that are capable of forming sp^3 hydrid orbitals (*32*).

The above model cannot be applied directly, however, to the results of the present study. For instance, Ti^{4+}, V^{5+}, and Mo^{6+} supported on silica showed the presence of substantial numbers of Brønsted acid sites. We will extend the above model to include these additional systems in the remainder of this paper.

The essential notion underlying the present model involves Pauling's electrostatic valence rule (57), which states that a stable ionic structure should result in a net charge balance equal to zero around each ion. Accordingly, the formal charge of an ion should equal the sum of the electrostatic bond strengths around it. An electrostatic bond strength for each bond corresponds to the charge of an ion divided by its coordination number.

The coordination number of Si^{4+} in SiO_2 is four. An electrostatic bond strength of 1 valence unit (v.u.) may be equally distributed for each Si–O bond. In the bulk of SiO_2, each oxygen anion is coordinated to two Si cations, which fulfills the charge balance requirement. However, surface oxygens may be bonded to only one Si ion. Since each oxygen strives for a formal valence of −2, such surface oxygens are undersaturated. Consequently, they would be stabilized by forming hydroxyl groups. The electrostatic bond strength of the resulting O–H bond is equal to 1 v.u. According to Pauling's logarithmic relationship relating the electrostatic bond strength to the covalency, this O–H bond is only 33% ionic (57). Hence, hydrogen atoms of surface Si–OH groups are not expected to be acidic.

Both Si and Al ions are generally believed to be tetrahedrally coordinated to oxygens in Al/SiO_2 samples. Each Al–O bond possesses an electrostatic bond strength of 0.75 v.u. Terminal hydroxyl groups bonded to Al ions on the surface lead to O–H bond strengths of 1.25 v.u., more covalent than those bonded to Si ions. Another type of the surface hydroxyl group is bridged between Si and Al ions. The sum of the electrostatic bond strengths from Al and Si is 1.75 v.u. Since the degree of undersaturation (0.25 v.u.) is relatively small for this bridging oxygen, it can remain undersaturated on the surface in the fully dehydrated state. However, when the surface is exposed to water vapor, protons created by the dissociation of water molecules would saturate such oxygens. The electrostatic bond strength of this O–H bond is 0.25 v.u., corresponding to an ionic character of 80%. This value indicates the protonic nature of the above type of hydrogens, and Brønsted acidity is expected.

The coordination number of a Zn ion in Zn/SiO_2 may be assumed to be four, since this cation is known to take tetrahedral coordination in most metal oxides and minerals. The undersaturation of terminal oxygens (1.5 v.u.) bonded to Zn ions is such that stable surface hydroxyls would be readily formed. The corresponding bond strength of 1.5 v.u. makes the O–H bond highly covalent. Bridging oxygens between Zn and Si ions show an undersaturation of 0.5 v.u., which may also attract protons to form hydroxyl groups. The resulting bond exhibits 65% ionicity, with a formal charge of +0.5 on hydrogen. Since no evidence for the presence of Brønsted acid sites was observed even in the presence of water for Zn/SiO_2, it can be suggested that a positive formal charge of 0.5 is not sufficient to lead to Brønsted acidity (as measured by pyridine adsorption).

In the case of Ti/SiO_2, two possibilities exist with respect to the coordination of Ti^{4+}. If tetrahedral coordination is assumed, the same conclusion can be reached as stated previously in the case of SiO_2 alone, for which no Brønsted acidity is expected. For octahedral coordination for Ti^{4+}, each Ti–O bond has an electrostatic bond strength of 0.67 v.u. The bond strength of 1.33 v.u. for terminal Ti–OH groups leads to highly covalent character. The bridging oxygens between Ti and Si ions are undersaturated by 0.33 v.u., which may form hydroxyl groups by attracting protons, giving +0.67 for the formal charge of hydrogen. From the experimental results, where substantial amounts of Brønsted acid sites were found for the oxidized form of Ti/SiO_2 upon exposure to water vapor, an undersaturation of 0.33 for surface oxygens can be considered to create Brønsted acidity.

For the reduced form of Ti/SiO_2, no evidence for Brønsted acid sites was observed. The oxidation state of a reduced Ti ion can be either Ti^{3+} or Ti^{2+} under the conditions studied, and these cations prefer octahedral environment. Following the procedure described above, the terminal Ti–OH group is evaluated to be highly covalent, and the formal charge for the hydrogen of the bridging hydroxyl group is +0.5 and +0.33 for Ti^{3+} and Ti^{2+}, respectively. As derived for Zn/SiO_2, none of these species would be expected to lead to Brønsted acid sites.

From the above discussion, it may be noted that the degree of undersaturation for surface oxygens is dependent only on the valence and the coordination of the cations, and that terminal hydroxyls are never expected to be acidic. A general criterion for the generation of Brønsted acidity may be established for a series of silica-supported metal oxides, provided that the cation in question is placed in an undistorted environment. The values for the undersaturation of oxygens bridging between Si^{4+} and various cation environments, along with the formal charge of the resulting hydroxyl group, are summarized in Table 1. The possible range for oxygen undersaturation that can induce Brønsted acidity has been tentatively assigned to be between 0.1 and 0.4 v.u., which corresponds to a formal charge of hydrogen from +0.9 to +0.6. The lower limit for oxygen undersaturation is determined based on the consideration that an electrostatic bond strength for an O–H bond less than 0.1 v.u. would not be strong enough to retain a proton. The higher limit is derived from experimental observations, according to which an undersaturation of 0.33 v.u. caused the formation of Brønsted acid sites, while that of 0.50 v.u. did not.

An approach similar to the present model has been described by Knözinger and Rathasamy to account for various kinds of hydroxyl configurations on alumina surfaces (*58*). The net charges of hydrogen atoms associated with surface hydroxyls were evaluated for possible combinations of cation coordination (tetrahedral or octa-

TABLE 1

Brønsted Acidity on Silica-Supported Metal Oxides for Cations in Undistorted Environment

Valence of cation	Coordination number	Bond strength[a] (v.u.)	Oxygen undersat.[b]	Formal charge on hydrogen	Brønsted acidity[c]
2	4	0.50	0.50	0.50	X
2	6	0.33	0.67	0.33	X
2	8	0.25	0.75	0.25	X
3	4	0.75	0.25	0.75	O
3	6	0.50	0.50	0.50	X
3	8	0.37	0.63	0.37	X
4	4	1.00	0.00	1.00	X
4	6	0.67	0.33	0.67	O
4	8	0.50	0.50	0.50	X
5	4	1.25	−0.25	1.25	X
5	6	0.83	0.17	0.83	O
5	8	0.63	0.37	0.63	O
6	4	1.50	−0.50	1.50	X
6	6	1.00	0.00	1.00	X
6	8	0.75	0.25	0.75	O

[a] Metal-to-oxygen bond strength of a doped cation.

[b] Undersaturation of bridging oxygen between a doped cation and a silicon ion.

[c] O, Brønsted acidity predicted; X, no Brønsted acidity predicted.

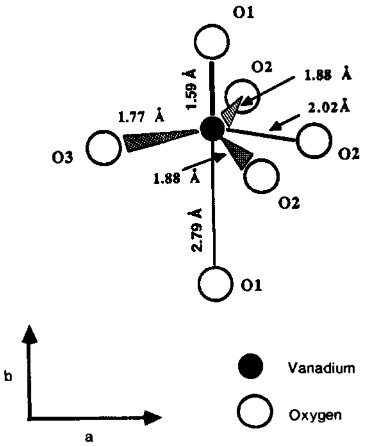

FIG. 7. V–O bond distances for V_2O_5 with the V ion in the center of a distorted octahedron (*40*).

hedral) and oxygen coordination (from one to three), and these charges were shown to be in the range from +0.5 to −0.5. According to our proposed model, none of these hydroxyl groups should exhibit Brønsted acidity, which is in agreement with the literature where no Brønsted acid sites have been reported to be present on alumina even in the presence of water vapor (e.g., (*24*)). Knözinger and Rathasamy also correlated the net charges for the surface hydroxyls to the infrared stretching frequencies. The absorption band at 3700–3710 cm^{-1} has been assigned to the most acidic hydroxyl groups with the charge of +0.5, and that at 3785–3800 cm^{-1} to the most basic hydroxyls with the charge of −0.5. Accordingly, hydrogen atoms of hydroxyl groups with charges greater than +0.5 would show infrared frequencies lower than 3700 cm^{-1}. In fact, Chu and Chang reported that B, Fe, and Ga ions incorporated into the tetrahedral framework of ZSM zeolites give hydroxyl stretching frequencies at 3610 cm^{-1} (*59*). In agreement with this observation, the hydrogen charge of bridging hydroxyl groups is calculated to be 0.75 according to the present model.

In the preceding discussion, the mean electrostatic bond strength as defined by Pauling has been employed. However, for cations in distorted environments, individual bond strengths should be calculated from the corresponding bond lengths. Various empirical relationships between bond length and bond strength have been proposed (e.g., (*60–62*)). The most rigorous and quantitative work was published by Brown *et al.* (*63, 64*). They derived a bond-strength–bond-length relationship for bonds between oxygen and different elements in various oxidation states, which is formulated as

$$s = (R/R_0)^{-N},$$

where s is the electrostatic bond strength, R is the bond length, and R_0 and N are constants given for each element. The usefulness of the Brown's relationship for cations with distorted coordination spheres has been inspired by the work of Andersson (*65*) and of Ziólkowski (*43*).

It is possible to use Brown's correlation to calculate for TiO_2 the electrostatic environments of possible configurations of surface oxygens in rutile, anatase, and their mixtures, as described in detail elsewhere (*36*). In short, no oxygen species with unsaturations between 0.1 and 0.4 v.u. are expected. This is consistent with the observation that a significant number of Brønsted acid sites were not observed on titania.

The coordination sphere of a vanadium cation in the structure of V_2O_5 can be viewed as either a distorted trigonal bipyramid or a distorted octahedron. The dimensions for the V–O bonds are shown in Fig. 7. There are three types of oxygens in the bulk of V_2O_5. One type of oxygen, O1, is essentially doubly bonded to a vanadium cation, with an electrostatic bond strength of 1.86 v.u. Oxygen O2 is coordinated to three vanadium cations. One of the three V–O2 bonds, forming a two-dimensional network parallel to the (010) plane, is longer than the other two bonds. Oxygen O3 links the bipyramids by sharing corners in the a and c directions.

Based on the V–O bond strengths calculated from the corresponding bond lengths

TABLE 2

Oxygen Undersaturations for V_2O_5

Type[a]	Coordination number	Sum of V–O bond strengths[b] (v.u.)	Oxygen undersat.[c] (v.u.)
O1	1	1.86	0.14
O2	1	0.54	1.46
		0.79	1.21
	2	1.33	0.67
		1.58	0.42
	3	2.11	−0.11
O3	1	1.03	0.97
	2	2.06	−0.06

[a] Type of oxygen. Corresponding V–O bond lengths are shown in Fig. 7.

[b] Calculated from Brown's formula; R_1 = 1.791, N = 5.1.

[c] Undersaturation.

using Brown's formula, possible values for oxygen undersaturations can be obtained for different coordination environments of oxygen. As shown in Table 2, two of the possible configurations satisfy the requirement for the occurrence of Brønsted acidity. A doubly bonded oxygen O1 located on the (010) face exhibits an undersaturation of 0.14 v.u. On the (101) plane, a two-coordinated O3 may be undersaturated by 0.42 v.u. Although this value exceeds the previously assigned upper limit (0.4 v.u.) for the generation of Brønsted acidity, such a slight difference is not significant. Since the predominant cleavage plane of V_2O_5 is the (010) face, it seems that oxygens with double-bond character are mainly responsible for the formation of Brønsted centers observed in the present study.

Ziólkowski has calculated the sums of Mo–O electrostatic bond strengths around oxygen atoms for various configurations on the surface using the Brown's bond-strength–bond-length relationship (*43*). These values are listed in Table 3 with the corresponding crystallographic planes. Among the possible configurations, surface oxygens with the sum of bond strengths of 1.90 and 1.63 v.u. (corresponding to oxygen undersaturations of 0.1 and 0.37 v.u.) are expected to show Brønsted acidity. The former doubly bonded oxygen sites are located on the (100) and (010) faces, and the latter sites are on the (100) and (101) faces. The layered structure of MoO_3 along the b direction exposes the (010) plane in preference to the other cleavage faces. Therefore, the observed Brønsted acidity is again considered to be mainly caused by doubly bonded oxygens on the (010) plane.

Finally, we do not have sufficient structural data to apply Brown's electrostatic formula to our silica-supported vanadia and molybdena samples. However, based on the above discussion, the presence of terminal, doubly bonded oxygens is probably important for the generation of Brønsted acid sites for the oxidized V/SiO_2 and Mo/SiO_2 materials. Indeed, Brønsted sites were not detected for reduced V/SiO_2 and Mo/SiO_2, even in the presence of water, and this may be due to the absence of terminal, doubly bonded oxygens for these samples.

CONCLUSIONS

The number of acid sites on Mo/SiO_2 and V/SiO_2 was shown to be greater than that

TABLE 3

Oxygen Undersaturations for MoO_3

Sum of Mo–O bond strengths[a] (v.u.)	Oxygen undersat.[b] (v.u.)	Crystallographic planes[c]
2.04	−0.04	(100) (001) (010) (101)
1.98	0.02	(001) (010)
1.90	0.10	(100) (010)
1.63	0.37	(100) (101)
1.09	0.91	(001) (101)
0.81	1.19	(001) (101)
0.34	1.66	(100)

[a] From Ref. (*43*); calculated from Brown's formula; R_1 = 1.882, N = 6.0.

[b] Undersaturation.

[c] From Ref. (*43*).

found for MoO_3 and V_2O_5 alone. The number of Lewis sites increased upon reduction by formation of oxygen vacancies on the surfaces. Silica-supported titania exhibited strong Lewis acidity, analogous to unsupported TiO_2.

The effects of water in the generation of Brønsted acid sites at the expense of Lewis sites were observed for some of the catalyst systems, including the oxidized forms of Ti/SiO_2, V/SiO_2, Mo/SiO_2, and Al/SiO_2. The effects were not significant for reduced surfaces of V/SiO_2, Mo/SiO_2, Ti/SiO_2, and oxidized Zn/SiO_2. A model accounting for the generation of Brønsted acidity has been proposed, which employs Pauling's electrostatic bond strength to evaluate the degree of undersaturation for surface oxygens. An undersaturation of 0.1–0.4 v.u. has been suggested to be capable of creating Brønsted acidity. It was demonstrated that metal-to-oxygen bond strengths calculated with Brown's empirical bond-strength–bond-length relationships may be substituted for Pauling's mean bond strengths for cations in highly distorted coordination environments. The importance of terminal, doubly bonded oxygens for vanadia and molybdena in creating Brønsted acid sites is also suggested. This concept is in agreement with recent quantum mechanical calculations (*66*).

ACKNOWLEDGMENTS

We acknowledge support from the Office of Basic Energy Sciences of the Department of Energy (Grant DE-FG02-84ER13183) for this work. We also acknowledge gratefully the Toho Titanium Co. for their financial support of T. Kataoka during this work. Finally, we thank N. Cardona-Martínez, B. Handy, L. Greppi, T. Srnak, S. Stevenson, and Dr. Masahiko Arai for valuable suggestions throughout this work.

REFERENCES

1. Anilin, B., and Fabrick, S., British Patent 1,140,264 (1969).

2. Vanhove, D., and Blanchard, M., *Bull. Soc. Chim. France*, 3291 (1971).

3. Gasior, M., Grzybowska, B., Haber, J., Machej, T., and Ziólkowski, J., *J. Catal.* **58,** 15 (1979).

4. Yoshida, S., Ueda, A., and Tarama, K., *Ind. Eng. Chem. Prod. Res. Dev.* **18,** 283 (1979).

5. Inomata, M., Miyamoto, A., Ui, T., Kobayashi, K., and Murakami, Y., *Ind. Eng. Chem. Prod. Res. Dev.* **21,** 424 (1982).

6. Liu, H. F., Liu, R. S., Liew, K. Y., Johnson, R. E., and Lunsford, J. H., *J. Amer. Chem. Soc.* **106,** 4117 (1984).

7. Zhen, K. J., Khan, M. M., Mak, C. H., Lewis, K. B., and Somorjai, G. A., *J. Catal.* **94,** 501 (1985).

8. Tanabe, K., *in* "Catalysis Science and Technology" (J. R. Anderson and M. Boudart, Eds.), Vol. 2, p. 231. Springer-Verlag, New York/Berlin, 1981.

9. Tanabe, K., "Solid Acids and Bases. Their Catalytic Applications." Academic Press, New York, 1970.

10. Benesi, H. A., and Winquist, B. H. C., *in* "Advances in Catalysis" (D. D. Eley, H. Pines, and P. B. Weisz, Eds.), Vol. 27, p. 98. Academic Press, New York, 1978.

11. Pohle, W., and Fink, P., *Z. Phys. Chem. N.F.* **109,** 77 (1978).

12. Morterra, C., Ghiotti, G., Boccuzzi, F., and Coluccia, S., *J. Catal.* **51,** 299 (1978).

13. Kermarec, M., Briend-Faure, M., and Delafosse, D., *J. Chem. Soc. Faraday Trans. 1* **70,** 2180 (1974).

14. Zecchina, A., Garrone, E., Ghiotti, G., and Coluccia, S., *J. Phys. Chem.* **79,** 972 (1975).

15. Van Roosmalen, A. J., Koster, D., and Mol, J. C., *J. Phys. Chem.* **84,** 3075 (1980).

16. Wendt, V. G., Gottschling, J., Standte, B., and Schöllner, R., *Z. Anorg. Allg. Chem.* **500,** 215 (1983).

17. Low, M. J. D., and Subba Rao, V. V., *Canad. J. Chem.* **46,** 3255 (1968).

18. Scokart, P. O., Declerck, F. D., Sempels, R. E., and Rouxhet, P. G., *J. Chem. Soc. Faraday Trans. 1* **73,** 359 (1977).

19. Scokart, P. O., and Rouxhet, P. G., *J. Colloid Interface Sci.* **86,** 96 (1982).

20. Lercher, J. A., *React. Kinet. Catal. Lett.* **20,** 409 (1982).

21. Riseman, S. M., Bandyopadhyay, S., Massoth, F. E., and Eyring, M., *Appl. Catal.* **16,** 29 (1985).

22. Lercher, J. A., Vinek, H., and Noller, H., *Appl. Catal.* **12,** 293 (1984).

23. Miyata, H., Nakagawa, Y., Ono, T., and Kubokawa, Y., *J. Chem. Soc. Faraday Trans. 1* **79,** 2343 (1983).

24. Kiviat, F. E., and Petrakis, L., *J. Phys. Chem.* **77,** 1232 (1973).

25. Mone, R., and Moscow, L., *Prepr. Amer. Chem. Soc. Div. Pet. Chem.* **20,** 564 (1975).

26. Mone, R., *in* "Preparation of Catalysts" (J. A. Delmon, P. A. Jacobs, and G. Poncelet, Eds.). Elsevier, New York, 1976.

27. Segawa, K., and Hall, W. K., *J. Catal.* **76,** 133 (1982).
28. Segawa, K., and Hall, W. K., *J. Catal.* **77,** 221 (1982).
29. Suarez, W., Dumesic, J. A., and Hill, C. G., Jr., *J. Catal.* **94,** 408 (1985).
30. Connell, G., and Dumesic, J. A., *J. Catal.* **101,** 103 (1986).
31. Connell, G., and Dumesic, J. A., *J. Catal.* **102,** 216 (1986).
32. Connell, G., and Dumesic, J. A., *J. Catal.* **105,** 285 (1987).
33. Parry, E. P., *J. Catal.* **2,** 371 (1963).
34. Santos, J., Phillips, J., and Dumesic, J. A., *J. Catal.* **81,** 147 (1983).
35. Chien, J. C. W., *J. Catal.* **23,** 71 (1971).
36. Kataoka, T., M.S. thesis, University of Wisconsin at Madison, 1987.
37. Tanaka, K., and White, J. M., *J. Phys. Chem.* **86,** 4708 (1982).
38. Belokopytov, Yu. V., Kholyavenko, K. M., and Gerei, S. V., *J. Catal.* **60,** 1 (1979).
39. Inomata, M., Miyamoto, A., and Murakami, Y., *J. Catal.* **62,** 140 (1980).
40. Bachmann, H. G., Ahmed, F. R., and Barnes, W. H., *Z. Kristallogr. Kristallgeometr. Kristallphys. Kristallchem.* **115,** 10 (1961).
41. Kepert, D. L., "The Early Transition Metals," p. 61. Academic Press, London/New York, 1972.
42. Goodenough, J. B., *in* "4th International Conference on the Chemistry and Uses of Molybdenum." Climax, 1982.
43. Ziółkowski, J., *J. Catal.* **84,** 317 (1983).
44. Kihlborg, L., *Ark. Kemi.* **21,** 357 (1963).
45. Shibata, K., Kiyoura, T., Kitagawa, J., Sumiyoshi, T., and Tanabe, K., *Bull. Chem. Soc. Japan* **46,** 2985 (1973).
46. Itoh, M., Hattori, H., and Tanabe, K., *J. Catal.* **35,** 225 (1974).
47. Marcinkowska, K., Rodrigo, L., Kaliaguine, S., and Roberge, P. C., *J. Catal.* **97,** 75 (1986).
48. Iwasawa, Y., and Yamagishi, M., *J. Catal.* **82,** 373 (1983).
49. Abdo, S., Clarkson, R. B., and Hall, W. K., *J. Phys. Chem.* **80,** 2431 (1976).
50. Hall, W. K., and Lo Jacono, M., "Proceedings, 6th International Congress on Catalysis, London, 1976" (G. C. Bond, P. B. Wells, and F. C. Tomkins, Eds.), p. 246. The Chemical Society, London, 1976.
51. Yermakov, Yu. I., *Catal. Rev. Sci. Eng.* **13,** 77 (1976).
52. Yermakov, Yu. I., Kuznetsov, B. N., and Ryndin, Yu. A., *J. Catal.* **42,** 73 (1976).
53. Lo Jacono, M., and Hall, W. K., *J. Colloid Interface Sci.* **58,** 76 (1977).
54. Weigold, H., *J. Catal.* **83,** 85 (1983).
55. Van Reijen, L. L., and Cossee, P., *Discuss. Faraday Soc.* **41,** 277 (1966).
56. Gates, B. C., Katzer, J. R., and Schuit, G. C. A., "Chemistry of Catalytic Processes." McGraw-Hill, New York, 1979.
57. Pauling, L. C., "The Nature of the Chemical Bond," 3rd ed. Cornell Univ. Press, Ithaca, NY, 1960.
58. Knözinger, H., and Rathasamy, P., *Catal. Rev. Sci. Eng.* **17**(1), 1 (1978).
59. Chu, C. T., and Chang, C. D., *J. Phys. Chem.* **89,** 1569 (1985).
60. Donnay, G., and Allman, R., *Amer. Min.* **55,** 1003 (1970).
61. Baur, W. H., *Trans. Amer. Crystallogr. Assoc.* **6,** 129 (1970).
62. Shannon, R. D., and Prewitt, C. T., *Acta Crystallogr. Sect. B* **25,** 925 (1969).
63. Brown, I. D., and Wu, K. K., *Acta Crystallogr. Sect. B* **32,** 1957 (1976).
64. Brown, I. D., and Shannon, R. D., *Acta Crystallogr. Sect. A* **29,** 266 (1973).
65. Andersson, A., *J. Solid State Chem.* **42,** 263 (1982).
66. Bernholc, J., Horsley, J. A., Murell, L. L., Sherman, L. G., and Soled, S., *J. Phys. Chem.* **91,** 1526 (1987).